**SUPPLEMENTARY FILES**

**Materials and Methods**

For silencing of *Emb*, *polo*, and *Z600/frs*, we used *P{TRiP.JF01311}* (BDSC#31358, Okazaki *et al*., 2020), *P{TRiP.GL00014}* (BDSC#35146, Peng *et al.,* 2015), and *P{TRiP.HMS00747}* (BDSC#32953, Ni *et al*., 2010), respectively. We also used *P{UASp-Polo$^{WT}$-GFP}* (a gift from V. Archambault. Montreal University, Montreal, Canada), *P{UASp-Wee1.VFP}2* (BDSC#65390), and *P{UASp-EGFP-Myt1}1* (BDSC#65393) for expressing the GFP tagged Polo, Wee1, or Myt1. *M{UAS-Z600.ORF.3xHA.GW}* (Fly-ORF#F002535) was used for ectopic expression of the HA-tagged Z600 protein in spermatocytes. For anti-Z600/Frs immunostaining, guinea pig anti-Z600/Frs antibody (Großhans, *et al*., 2003, a gift from J. Großhans (The Philipps University of Marburg, Marburg, Germany)) was used.

**References**

1. Peng F, Zhao Y, Huang X, Chen C, Sun L, Zhuang L, Xue L. (2015). Loss of Polo ameliorates APP-induced Alzheimer's disease-like symptoms in Drosophila. Sci. Rep. 5:16816.

2. Ni, J.Q., Zhou, R., Czech, B., Liu, L.P., Holderbaum, L., Yang-Zhou, D., Shim, H.S., Handler, D., Karpowicz, P., Binari, R., Booker, M., Brennecke, J., Perkins, L.A., Hannon, G.J., Perrimon, N. (2010). A genome-scale shRNA resource for transgenic RNAi in *Drosophila*. (Personal communication to FlyBase)

3. Großhans, J., Muller, H.A., Wieschaus, E. (2003). Control of cleavage cycles in Drosophila embryos by fruhstart. Dev. Cell 5(2): 285-294.

**Supplementary figure legends**

**Fig. S1. Effect of ectopic expression of normal CycB or NLS-CycB on their subcellular localization in mature spermatocytes.**

(A-P) Anti-CycB immunostaining of spermatocytes at S5 (A, D, F, I, L, O), S6 (B, E, G, J, M, P), and Prophase I (Pro) (C, H, K, N). The immunofluorescence was observed in normal spermatocytes (A-C), the cells expressing normal CycB (F-H) or NLS-CycB (L-N), *Nup62*-depleted spermatocytes (D, E), the depleted cells expressing normal CycB (I-K) or NLS-CycB (O, P). Spermatocytes expressing normal CycB or NLS-CycB, both of which are fused with HA tag, were simultaneously immunostained with anti-HA antibody. Anti-CycB immunofluorescence (red in A-P, white in A'-P'), Sa-GFP fluorescence to determine the stages of growth phase (green in A-P, white in A''-E'' and F''''-P''''), DNA staining with DAPI (blue in A-P, white in A'''-P'''), anti-HA immunofluorescence (green in F-P, white in F''-P''), and phase-contrast images (F'''''-P'''''). Scale bar: 10μm.

**Fig. S2. Intracellular localization of Wee1 and Myt1, and their close association with Cdk1 by *in situ* PLA in mature spermatocytes at S5, S6, and ProI.**

(A-F) Fluorescent images of spermatocytes expressing Wee1-GFP (A-C) or Myt1-GFP (D-F) at S5 (A, D), S6 (B, E), and Prophase I (Pro) (C, F) stages. Wee1-GFP fluorescence (green in A-C, white in A'-C'), Myt1-GFP fluorescence (green in D-F, white in D'-F'), DNA staining with DAPI (magenta in A-F, white in A''-F''). Scale bar: 10 μm. (G-J) Detection of protein complexes containing Cdk1 and Wee1 or Myt1 by *in situ* PLA in the spermatocytes expressing Wee1-GFP (G, H) or Myt1-GFP (I, J) at premeiotic stages using ant-Cdk1 and anti-GFP antibodies. Scale bar: 10 μm.

**Fig. S3. The effect of *polo*-silencing in spermatocytes on the G2/M progression in male meiosis.**

(A) A single intact cyst of spermatids in testis harboring the *polo*-silenced spermatocytes (*bam* >

*poloRNAi*). A phase-contrast image of spermatids stained with DAPI (red). The spermatid cyst consists of 16 cells (10 cysts / 10 cysts examined). Each of the spermatids contains a Nebenkern and 4 small nuclei for each (86% of 99 cysts examined). (B-D) Anti-MPM2 immunostaining of *polo*-silenced spermatocytes at S5 (B), S6 (C), and ProI (D). Anti-MPM2 immunostaining (red in B-C, white in B'-D'), Sa-GFP fluorescence (green in B-C, white in B''-D''), and DNA staining with DAPI (blue in B-D, white in B'''-D'''). Scale bar: 10μm.

**Fig. S4. Subcellular localization of Polo-GFP in spermatocytes from S5 of the growth phase to the later ProI.**

(A-H) Anti-CycB immunostaining of spermatocytes expressing GFP-tagged Polo at S5 (A, G), S6 (B, H), and ProI (C-F) with the progression of meiosis. The immunofluorescence was observed in normal spermatocytes (*bam* > *Polo-GFP*) (A-F) and *Nup62*-silenced spermatocytes (*bam* > *Nup62RNAi, Polo-GFP*) (G, H). GFP fluorescence of Polo-GFP (green in A-H, white in A'-H'), anti-CycB immunostaining (red in A-H, white in A''-H''), and DNA staining with DAPI (blue in A-H, white in A'''-H'''). Scale bar: 10μm.

**Fig. S5. Examination of protein interaction between CycB and Polo-GFP by *in situ* proximity ligation assay (PLA).**

(A-D) *In situ* PLA to detect the protein complexes containing CycB and Polo in the spermatocytes expressing Polo-GFP at S5 (A, D), S6 (B, E), and ProI (C) using anti-CycB and GFP antibodies. Normal spermatocytes (*bam* > *Polo-GFP*) (A-C) and *Nup62*-depleted spermatocytes (*bam* > *Nup62RNAi, Polo-GFP*) (D, E). Scale bar: 10μm.

**Fig. S6. Intracellular localization of Z600 protein in normal and *Nup62*-silenced spermatocytes**

**at mature stages, and immunostaining to detect colocalization of Z600 and CycB in the premeiotic cells.**

(A-E) Immunostaining of mature spermatocytes with anti-Z600 antibody. Normal control (A-C), and *Z600*-silenced (D-E) or *Nup62*-silenced (F) spermatocytes. Immunofluorescence of the cells with anti-Z600 antibody (red in A-F, white in A'-F'), Sa-GFP fluorescence (green in A-E, white in A''-E''), DNA staining with DAPI (blue in A-F, white in A'''-E''', F''), and phase-contrast images (A''''-E'''', F'''). (D, E) Anti-Z600 immunostaining of the *Z600*-silenced cells at S5 (D) and S6 (E) shows a faint signal at the background level. Scale bar: 10μm. (G, H) Simultaneous immunostaining of premeiotic spermatocytes with anti-HA and anti-CycB antibodies at S5 (G) and S6 (H) stages. Anti-HA immunostaining (red in G, H, white in G', H'), anti-CycB immunostaining (green in G, H, white in G'', H''), DNA staining with DAPI (blue in G, H, white in G''', H'''), Sa-GFP fluorescence (white in G'''', H''''), and phase-contrast images (G''''', H'''''). Scale bar: 10μm.

**Fig. S7. Single intact cysts of spermatids at onion stage in the testes harboring spermatocyte-specific depletion of components required for the nucleo-cytoplasmic transport.**

(A-D) Phase-contrast images of intact cysts consisting of spermatids harboring round Nebenkerns from control testis (A) or testes with spermatocytes-specific silencing of *Nup62* (B), *emb* (C), or *Fs(2)Ket* (D). DNA staining with DAPI (red). Scale bar: 10μm.

Yamazoe., et al

Figure. S1

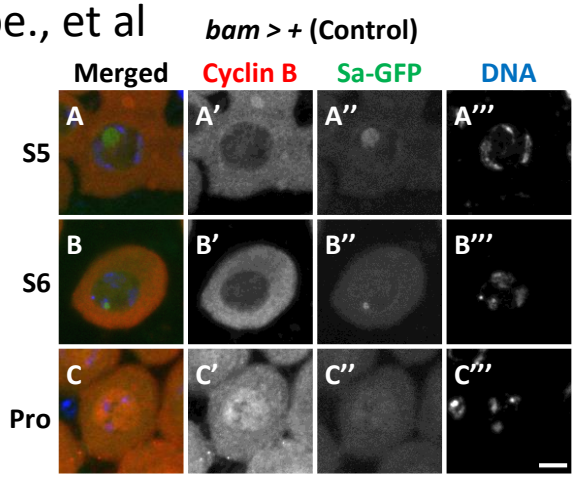


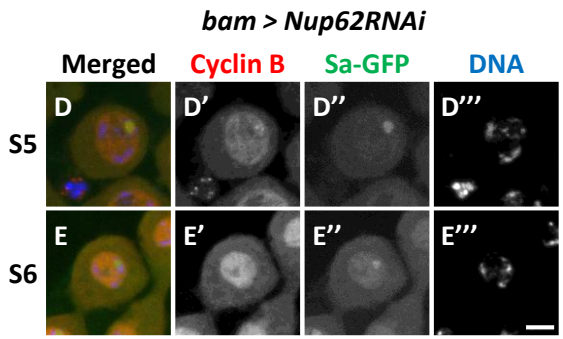


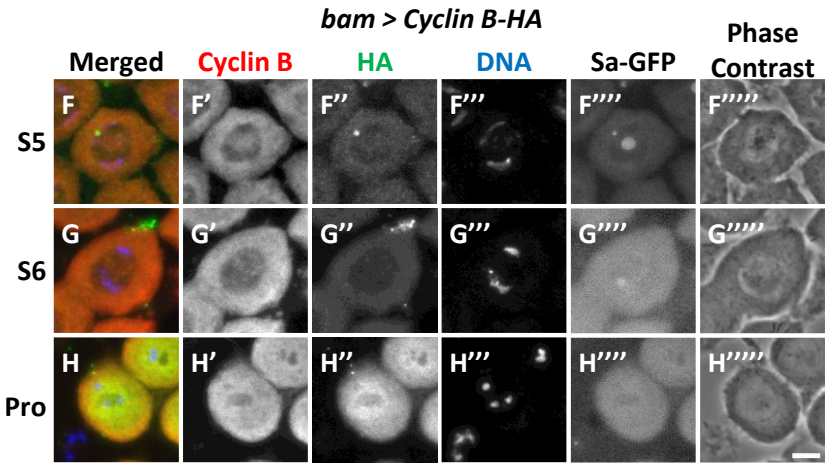


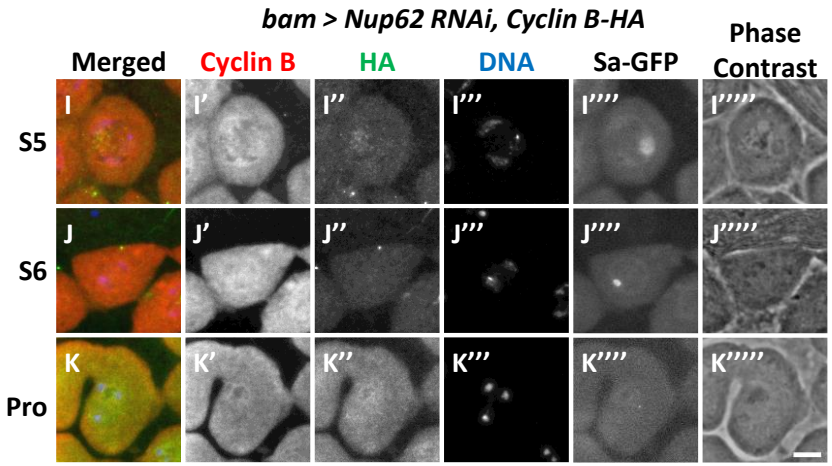


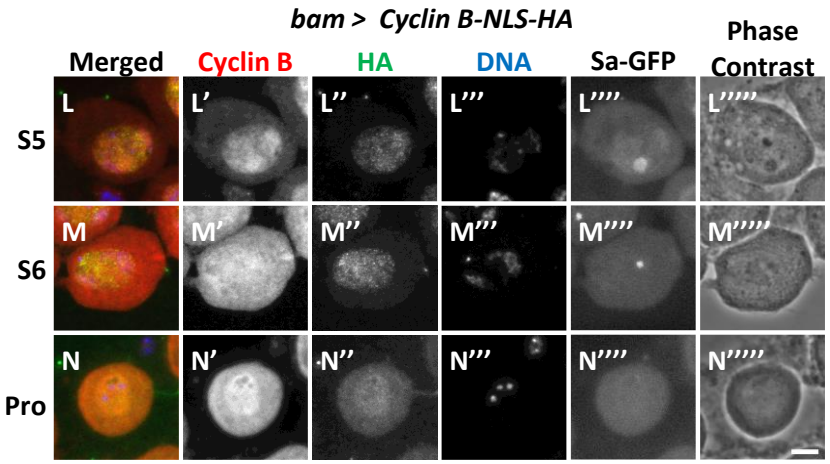


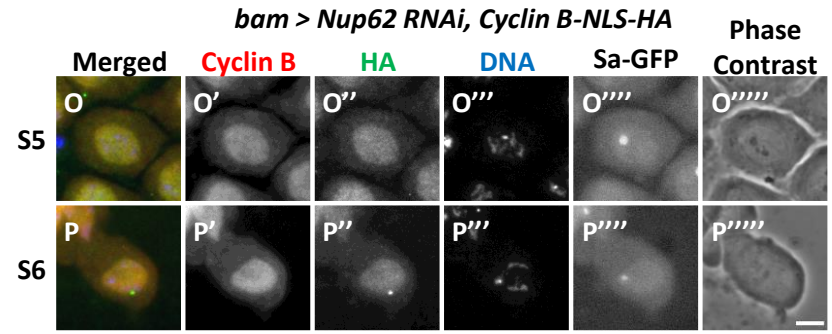

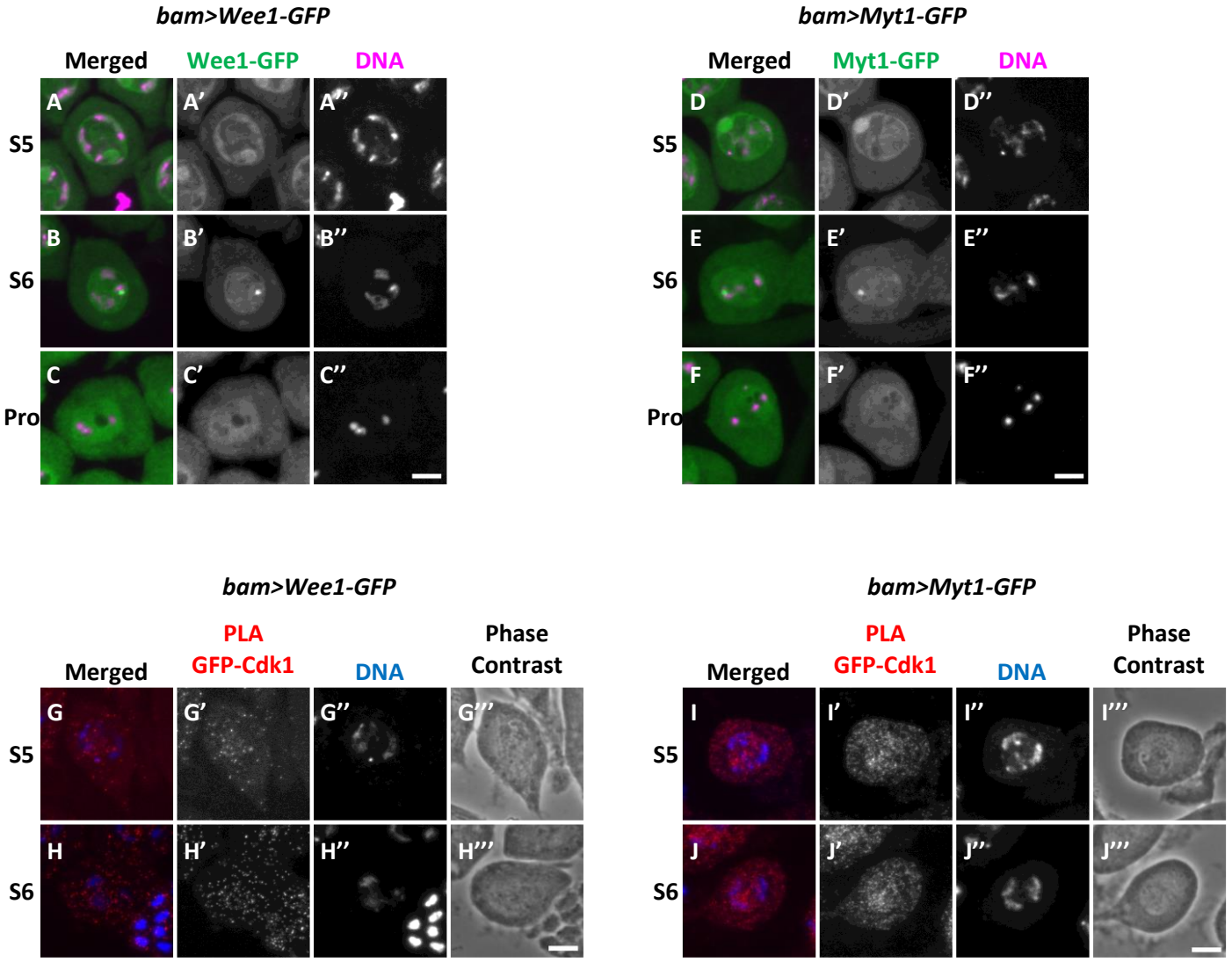
bam>Wee1-GFP
Merged
Wee1-GFP
DNA
S5
S6
Pro
A
A'
A''
B
B'
B''
C
C'
C''
bam>Myt1-GFP
Merged
Myt1-GFP
DNA
S5
S6
Pro
D
D'
D''
E
E'
E''
F
F'
F''
bam>Wee1-GFP
Merged
PLA
GFP-Cdk1
DNA
Phase
Contrast
S5
S6
G
G'
G''
G'''
H
H'
H''
H'''
bam>Myt1-GFP
Merged
PLA
GFP-Cdk1
DNA
Phase
Contrast
S5
S6
I
I'
I''
I'''
J
J'
J''
J'''

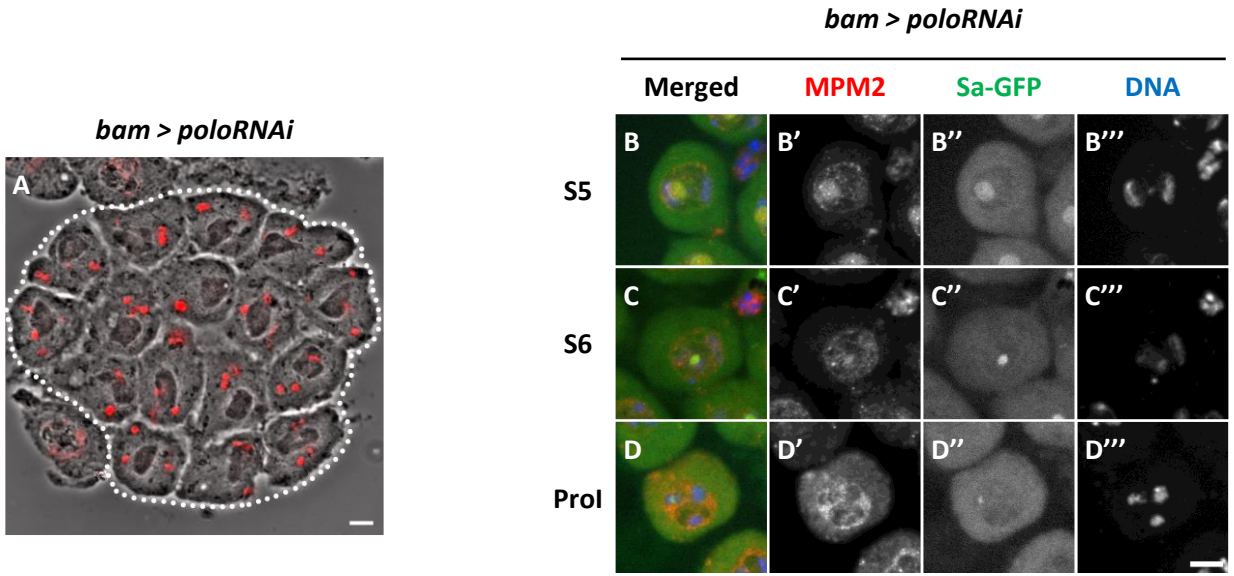
bam > poloRNAi
A
bam > poloRNAi
Merged
MPM2
Sa-GFP
DNA
S5
S6
ProI
B
B'
B''
B'''
C
C'
C''
C'''
D
D'
D''
D'''

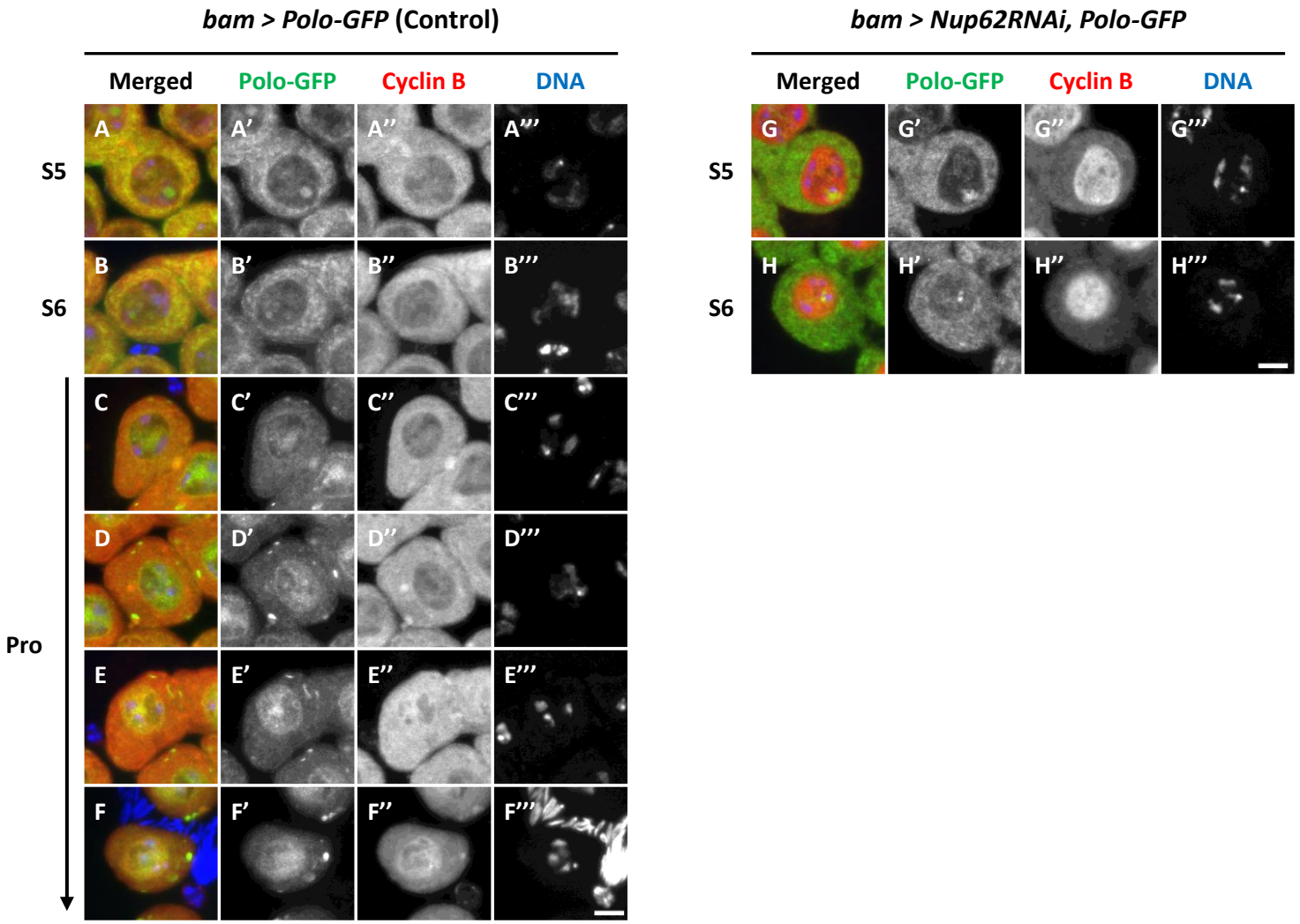
bam > Polo-GFP (Control)
bam > Nup62RNAi, Polo-GFP
Merged
Polo-GFP
Cyclin B
DNA
S5
S6
Pro
A
A'
A''
A'''
B
B'
B''
B'''
C
C'
C''
C'''
D
D'
D''
D'''
E
E'
E''
E'''
F
F'
F''
F'''
G
G'
G''
G'''
H
H'
H''
H'''

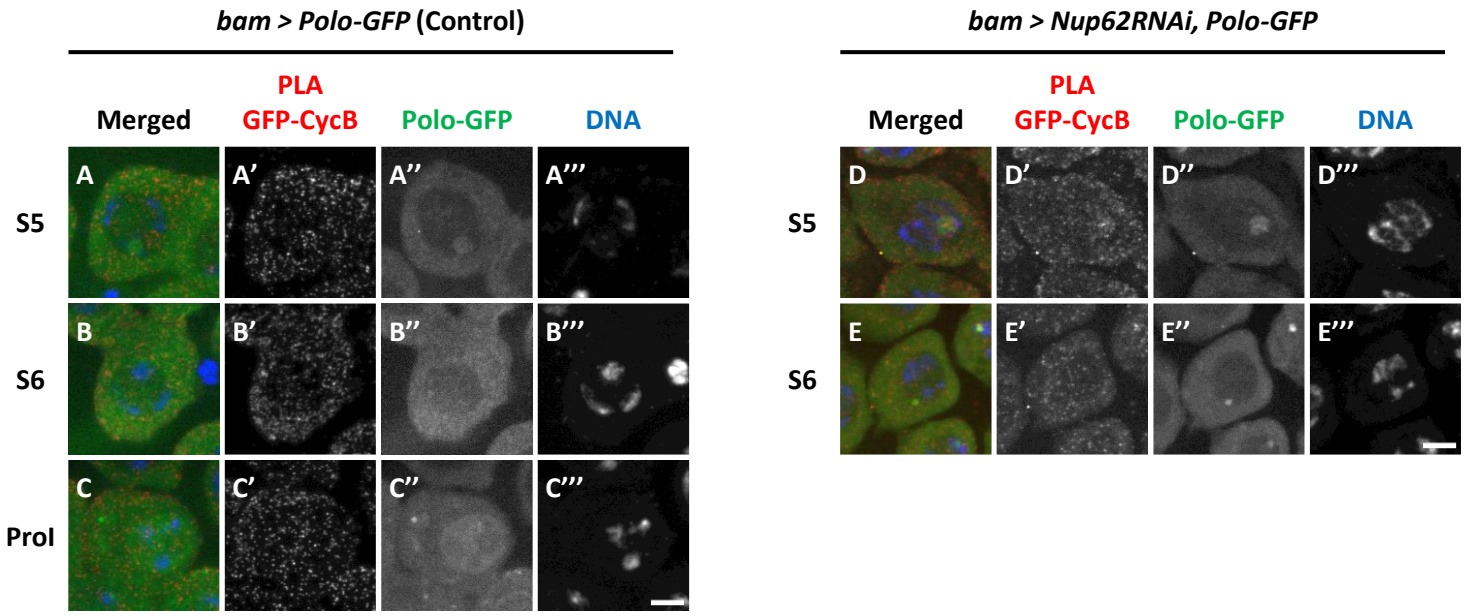
bam > Polo-GFP (Control)
bam > Nup62RNAi, Polo-GFP
Merged
PLA
GFP-CycB
Polo-GFP
DNA
S5
S6
Prol
A
A'
A''
A'''
B
B'
B''
B'''
C
C'
C''
C'''
D
D'
D''
D'''
E
E'
E''
E'''

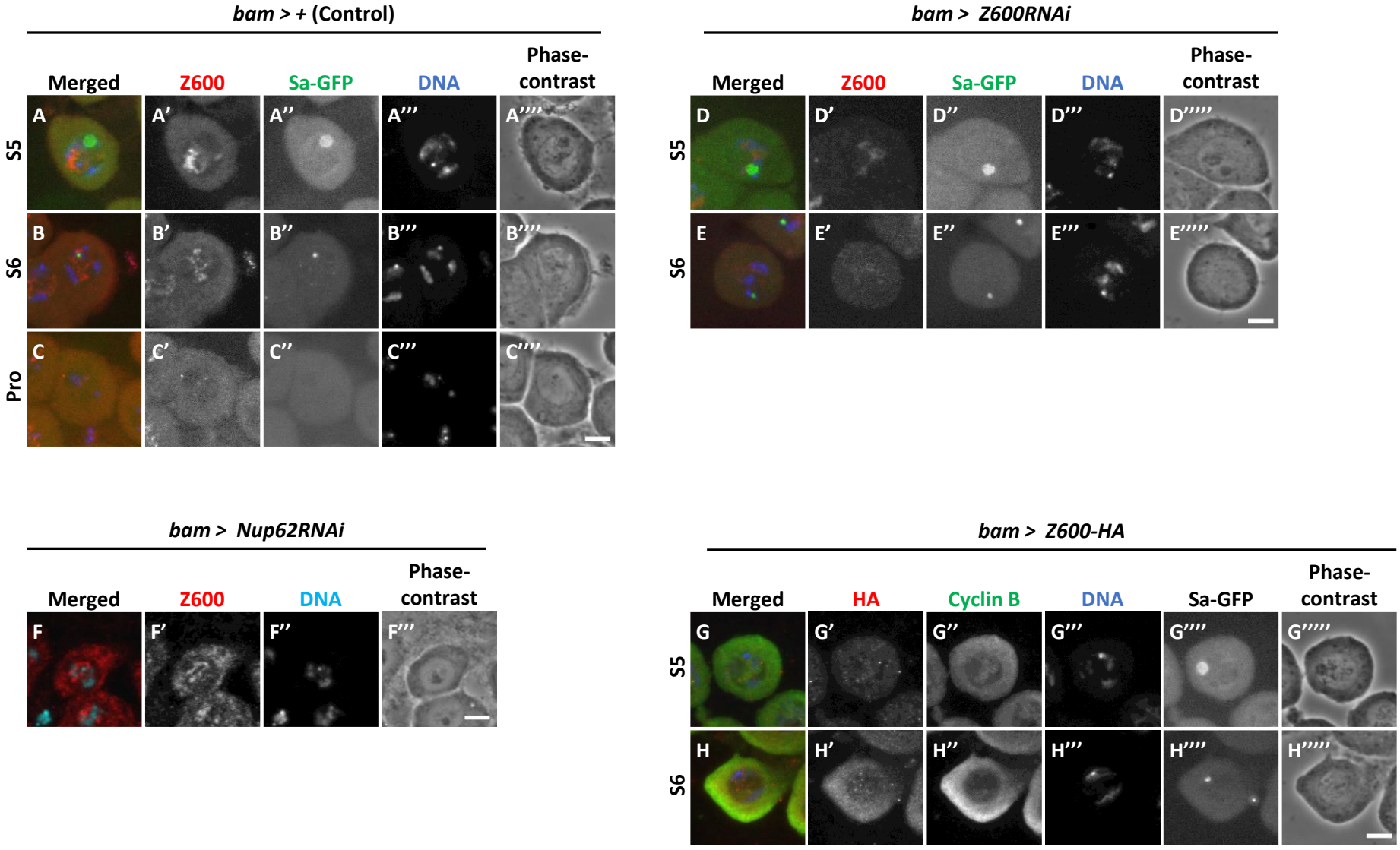
bam > + (Control)
Merged
Z600
Sa-GFP
DNA
Phase-contrast
S5
S6
Pro
A
A'
A''
A'''
A''''
B
B'
B''
B'''
B''''
C
C'
C''
C'''
C''''
bam > Z600RNAi
D
D'
D''
D'''
D'''''
E
E'
E''
E'''
E'''''
bam > Nup62RNAi
F
F'
F''
F'''
bam > Z600-HA
HA
Cyclin B
G
G'
G''
G'''
G''''
G'''''
H
H'
H''
H'''
H''''
H'''''

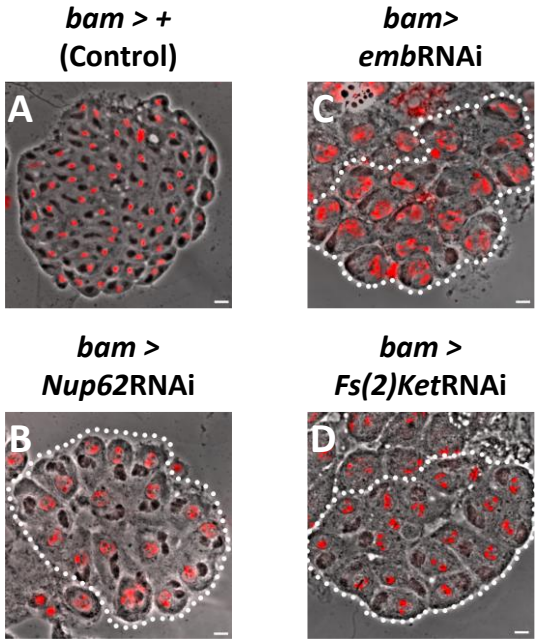
bam > +
(Control)
bam>
embRNAi
A
C
bam >
Nup62RNAi
bam >
Fs(2)KetRNAi
B
D